

SECOND ORDER ACCURATE UPWIND SOLUTIONS OF THE 2D STEADY EULER EQUATIONS BY THE USE OF A DEFECT CORRECTION METHOD

S.P.Spekreijse

*CWI, Centre for Mathematics and Computer Science
P.O.Box 4079, 1009 AB Amsterdam, The Netherlands*

ABSTRACT

In this paper a description is given of first and second order finite volume upwind schemes for the 2D steady Euler equations in generalized coordinates. These discretizations are obtained by projection-evolution stages, as suggested by Van Leer. The first order schemes can be solved efficiently by multigrid methods. Second order approximations are obtained by a defect correction method. In order to maintain monotone solutions, a limiter is introduced for the defect correction method.

1. INTRODUCTION

The steady state equations of inviscid flow, the steady Euler equations, are a nonlinear nonelliptic system of equations admitting solutions with discontinuities (shocks, contact discontinuities).

An important class of difference schemes for the (steady) Euler equations are the first order upwind schemes. These schemes are found by subdividing the domain of interest in disjunct control volumes (finite volume technique) and by assuming that the states in the volumes (or cells) are uniform (piecewise constant approximation). Then at each cell boundary two uniform states meet in a discontinuity. A unique flux, in the literature called the numerical flux [6], can be assigned after resolving the discontinuity by a set of elementary waves moving normal to the cell boundary or, in other words, after solving the one-dimensional Riemann-problem. This may be done exactly (Godunov [5]) or approximately (Osher [11], Roe [12], Van Leer [15], Steger & Warming [13]). The only difference between these schemes is the way of approximating the Riemann-problem. Therefore each first order upwind scheme is characterized by its numerical flux function.

Successful application of the multigrid method for the solution of the nonlinear system obtained by first order upwind schemes has been reported by Mulder & Van Leer [10],[18] and Hemker & Spekreijse [8],[9]. They use respectively Van Leer's and Osher's approximate Riemann-solver.

The purpose of this paper is to improve solutions of first order upwind schemes. This is highly

desirable because solutions of these schemes have some important shortcomings. Because of the hidden viscosity in these schemes, oblique (with respect to the mesh) shocks and contact discontinuities are smeared out disastrously. Furthermore, in the smooth part of the flow field the solution is only first order accurate, which is too low for practical purposes. Therefore we wish to improve the order of accuracy and to steepen oblique discontinuities without introducing over- or undershoot.

In the literature many second order upwind schemes with flux limiters are available [14],[17],[3],[1]. Without a flux limiter solutions of second or higher order schemes suffer from oscillations in the neighbourhood of discontinuities. Therefore flux limiters have been constructed and implemented in these schemes to prevent these oscillations. Such schemes, with their time dependent term, belong to the class of total variation diminishing (TVD) schemes [14]. The steady state solution of a second order TVD scheme possesses the improvements we wish to obtain.

The construction of time dependent first or second order (TVD) upwind schemes can be considered most conveniently (as suggested by Van Leer [16],[1]) in two stages: a projection stage and an evolution stage (MUSCL-approach). In the projection stage the states in the cells are interpolated to yield approximations of the states at the cell boundaries. If this approximation is made by extrapolation from both sides of a cell boundary then two uniform states meet in a discontinuity. In the evolution stage, at each cell boundary, an approximate Riemann solver (or equivalently a numerical flux function) is used to calculate the flux from these two uniform states. When a second order upwind scheme is constructed by this method, a flux limiter, developed to make the scheme TVD, only needs to be applied in the projection stage.

Because the solution of first order upwind schemes can be obtained efficiently (by the multigrid method), it seems that an iterative defect correction (DeC) method provides a simple way to obtain the steady state solution of a second order TVD scheme. Unfortunately however, such an iterative DeC process will converge very slowly or might not even converge at all. On the other hand, it is well known [2] that just one or more DeC iterations are enough to obtain a second order accurate approximation. Therefore we shall apply the DeC iteration steps only a few times. This makes the method cheap to apply but it also implies that the steady state solution of the second order TVD scheme will not be achieved. The flux limiter, developed to make the second order upwind scheme TVD, only ensures that the steady state solution will be monotone and not that a second order approximation obtained after a few DeC iteration steps is monotone as well. It is practical experience that wiggles may occur after a few defect corrections despite the use of a flux limiter. Therefore in the context of the DeC method, it is not appropriate to use a flux limiter.

On the other hand, after each DeC iteration step the new solution can be considered as the sum of the solution of the first order upwind scheme plus a correction. In order to prevent that the addition of the correction to the first order solution creates new local extrema (wiggles), this correction has to be modified (limited!). The modification of the correction is one of the main topics of this paper. Because the first order upwind scheme is a monotone scheme, this strategy ensures that after each DeC iteration step the solution will stay monotone, or in other words no over- or undershoot will occur. Shortly, we suggest to apply a limiter in the DeC method and not in the second order upwind scheme.

In section 2 we describe the first and second order upwind discretization of the 2D steady Euler equations in general geometries. The subdivision of the discretization by the projection and evolution stages is applied. A proof is given of the accuracy of these discretizations.

In section 3 the DeC method is described. A description of a simple limiter used in the DeC method is given.

In section 4 some numerical results concerning the resolution of a contact discontinuity and an oblique shock are presented.

2. SECOND ORDER FINITE VOLUME UPWIND DISCRETIZATION OF THE 2D STEADY EULER EQUATIONS

The 2D Euler equations can be written in conservative-vector form as

$$\frac{\partial}{\partial t} q + \frac{\partial}{\partial x} f(q) + \frac{\partial}{\partial y} g(q) = 0, \quad (2.1)$$

on an open (irregular) domain $\Omega^* \subset \mathbb{R}^2$, where

$$q = \begin{bmatrix} \rho \\ \rho u \\ \rho v \\ e \end{bmatrix}, \quad f(q) = \begin{bmatrix} \rho u \\ \rho u^2 + p \\ \rho uv \\ u(e+p) \end{bmatrix}, \quad g(q) = \begin{bmatrix} \rho v \\ \rho uv \\ \rho v^2 + p \\ v(e+p) \end{bmatrix}. \quad (2.2)$$

Here, respectively ρ, u, v, p and e are density, velocity components in the x - and y -directions, pressure and total energy per unit volume. Furthermore, e may be expressed as

$$e = \rho(\epsilon + \frac{1}{2}(u^2 + v^2)), \quad (2.3)$$

where the specific internal energy ϵ , is related to the pressure and density by the perfect gas law

$$p = (\gamma - 1)\rho\epsilon, \quad (2.4)$$

with γ denoting the ratio of specific heats.

The physical domain Ω^* is subdivided into disjunct quadrilateral cells $\Omega_{i,j}^*$, $(i,j) \in \{1..M, 1..N\}$ in a regular fashion such that

i) $\Omega^* = \bigcup_{i,j} \Omega_{i,j}^*$,

ii) $\Omega_{i,j}^*$, $\Omega_{i\pm 1,j}^*$, $\Omega_{i,j\pm 1}^*$ are neighbouring cells,

iii) $(x_{i+\frac{1}{2},j+\frac{1}{2}}, y_{i+\frac{1}{2},j+\frac{1}{2}}) = \bar{\Omega}_{i,j}^* \cap \bar{\Omega}_{i+1,j}^* \cap \bar{\Omega}_{i,j+1}^* \cap \bar{\Omega}_{i+1,j+1}^*$ is a common vertex of the cells $\Omega_{i,j}^*$, $\Omega_{i+1,j}^*$, $\Omega_{i,j+1}^*$ and $\Omega_{i+1,j+1}^*$.

It is clear that the vertices $\{(x_{i+\frac{1}{2},j+\frac{1}{2}}, y_{i+\frac{1}{2},j+\frac{1}{2}})\}$ define the subdivision of Ω^* completely.

Let (ξ, η) and (x, y) denote the cartesian coordinates in respectively the computational and physical space. In the computational space, we consider a rectangular domain Ω subdivided into equidistant square control volumes (or cells) $\Omega_{i,j}$, $(i,j) \in \{1..M, 1..N\}$ in such a way that $(h \cdot i, h \cdot j)$ is the mid-point of $\Omega_{i,j}$; h denotes the length of the edges. Assume the existence of a sufficiently smooth 1-1 relation between (ξ, η) and (x, y) :

$$\begin{cases} \xi = \xi(x, y) \\ \eta = \eta(x, y) \end{cases} \Leftrightarrow \begin{cases} x = x(\xi, \eta) \\ y = y(\xi, \eta) \end{cases}, \quad (2.5)$$

such that each cell $\Omega_{i,j}$ corresponds with $\Omega_{i,j}^*$ by this mapping i.e. for all $(i,j) \in \{0..M, 0..N\}$

$$(x_{i+\frac{1}{2},j+\frac{1}{2}}, y_{i+\frac{1}{2},j+\frac{1}{2}}) = (x(\xi_{i+\frac{1}{2}}, \eta_{i+\frac{1}{2}}), y(\xi_{i+\frac{1}{2}}, \eta_{i+\frac{1}{2}})), \quad (2.6)$$

where $\xi_{i+\frac{1}{2}} = (i + \frac{1}{2}) \cdot h$ and $\eta_{j+\frac{1}{2}} = (j + \frac{1}{2}) \cdot h$. It can be easily seen that in the computational space (ξ, η) the Euler equations become

$$\frac{\partial}{\partial t} (Jq) + \frac{\partial}{\partial \xi} (y_\eta f(q) - x_\eta g(q)) + \frac{\partial}{\partial \eta} (x_\xi g(q) - y_\xi f(q)) = 0, \quad (2.7)$$

with $J = x_\xi y_\eta - y_\xi x_\eta$.

The discretization of (2.1) on Ω^* is equivalent with the discretization of (2.7) on Ω . Because Ω is a rectangle subdivided into equidistant cells of length h , it is easier to obtain first and second order

upwind discretizations of (2.7) on Ω than of (2.1) on Ω^* . In symbolic form we write (2.7) as

$$(Jq)_t + N(q) = 0, \tag{2.8}$$

and the steady Euler equations as

$$N(q) = 0, \tag{2.9}$$

Here $N: X \rightarrow Y$ is a nonlinear operator, $X \subset [L^2(\Omega)]^4$ is the space of possible fluid states and $Y = [L^2(\Omega)]^4$ is the Banach space of rates of change (of states).

Define the finite dimensional vector spaces X_h and Y_h by

$$X_h = Y_h = \{q_{i,j} \in \mathbb{R}^4 \mid i = 1..M, j = 1..N\}. \tag{2.10}$$

The relation between the spaces X and X_h , Y and Y_h is obtained by introducing $R_h : X \rightarrow X_h$ and $\bar{R}_h : Y \rightarrow Y_h$

$$(R_h q)_{i,j} = (\bar{R}_h q)_{i,j} = \frac{1}{h^2} \iint_{\Omega_{i,j}} q(\xi, \eta) d\xi d\eta, \tag{2.11}$$

for any $q \in [L^2(\Omega)]^4$. Thus $(R_h q)_{i,j}$ is the mean value of q in $\Omega_{i,j}$. A p -order accurate discretization of (2.9) is an associated problem

$$N_h^p(q) = 0, \tag{2.12}$$

where $N_h^p : X_h \rightarrow Y_h$ has the property that for all sufficiently smooth $q \in X$

$$(N_h^p R_h q)_{i,j} - (\bar{R}_h N q)_{i,j} = O(h^p). \tag{2.13}$$

In this paper we will consider first and second order upwind schemes, so $p=1$ or $p=2$.

Notice that

$$\begin{aligned} (\bar{R}_h N q)_{i,j} = \frac{1}{h^2} \cdot \{ & \int_{\Gamma_{i+\frac{1}{2},j}} (y_\eta f - x_\eta g)(q((i + \frac{1}{2}) \cdot h, \eta)) d\eta - \\ & \int_{\Gamma_{i-\frac{1}{2},j}} (y_\eta f - x_\eta g)(q((i - \frac{1}{2}) \cdot h, \eta)) d\eta + \int_{\Gamma_{i,j+\frac{1}{2}}} (x_\xi g - y_\xi f)(q(\xi, (j + \frac{1}{2}) \cdot h)) d\xi - \\ & \int_{\Gamma_{i,j-\frac{1}{2}}} (x_\xi g - y_\xi f)(q(\xi, (j - \frac{1}{2}) \cdot h)) d\xi \}, \end{aligned} \tag{2.14}$$

where $\Gamma_{i+\frac{1}{2},j}, \Gamma_{i-\frac{1}{2},j}, \Gamma_{i,j+\frac{1}{2}}, \Gamma_{i,j-\frac{1}{2}}$ denote the boundaries of cell $\Omega_{i,j}$, defined by $\Gamma_{i+\frac{1}{2},j} = \bar{\Omega}_{i,j} \cap \bar{\Omega}_{i+1,j}, \Gamma_{i,j+\frac{1}{2}} = \bar{\Omega}_{i,j} \cap \bar{\Omega}_{i,j+1}$ etc.

Now we will construct an operator $N_h : X \rightarrow Y_h$, easier to approximate than $\bar{R}_h N$, but such that for all sufficiently smooth $q \in X$

$$(\tilde{N}_h q)_{i,j} - (\bar{R}_h N q)_{i,j} = O(h^2). \tag{2.15}$$

If we are able to construct $N_h^p : X_h \rightarrow Y_h, p = 1, 2$ such that

$$(N_h^p R_h q)_{i,j} - (\tilde{N}_h q)_{i,j} = O(h^p), \tag{2.16}$$

then also

$$(N_h^p R_h q)_{i,j} - (\bar{R}_h N q)_{i,j} = O(h^p). \tag{2.17}$$

This means that after the construction of a \tilde{N}_h satisfying (2.15) we may restrict ourselves to the approximation of \tilde{N}_h instead of $\bar{R}_h N$. An obvious choice for the operator N_h is

$$(\tilde{N}_h q)_{i,j} = \frac{1}{h} \cdot \{ (y_{\eta_{i+\frac{1}{2},j}} f - x_{\eta_{i+\frac{1}{2},j}} g)(\bar{q}_{i+\frac{1}{2},j}) - (y_{\eta_{i-\frac{1}{2},j}} f - x_{\eta_{i-\frac{1}{2},j}} g)(\bar{q}_{i-\frac{1}{2},j}) \}$$

$$+ (x_{\xi_{j+n}} g - y_{\xi_{j+n}} f)(\bar{q}_{i,j+\frac{1}{2}}) - (x_{\xi_{j-n}} g - y_{\xi_{j-n}} f)(\bar{q}_{i,j-\frac{1}{2}}) \}, \quad (2.18)$$

where

$$\begin{aligned} y_{\eta_{j+n}} &= \frac{1}{h} (y_{i+\frac{1}{2},j+\frac{1}{2}} - y_{i+\frac{1}{2},j-\frac{1}{2}}), & x_{\eta_{j+n}} &= \frac{1}{h} (x_{i+\frac{1}{2},j+\frac{1}{2}} - x_{i+\frac{1}{2},j-\frac{1}{2}}), \\ x_{\xi_{j+n}} &= \frac{1}{h} (x_{i+\frac{1}{2},j+\frac{1}{2}} - x_{i-\frac{1}{2},j+\frac{1}{2}}), & y_{\xi_{j+n}} &= \frac{1}{h} (y_{i+\frac{1}{2},j+\frac{1}{2}} - y_{i-\frac{1}{2},j+\frac{1}{2}}), \end{aligned} \quad (2.18a)$$

and

$$\bar{q}_{i+\frac{1}{2},j} = \frac{1}{h} \int_{\Gamma_{i+\frac{1}{2},j}} q((i+\frac{1}{2})h, \eta) d\eta. \quad (2.18b)$$

Thus $\bar{q}_{i+\frac{1}{2},j}$ is the mean value of $q(\xi, \eta)$ at the cell boundary $\Gamma_{i+\frac{1}{2},j}$. In a similar way $\bar{q}_{i-\frac{1}{2},j}$, $\bar{q}_{i,j+\frac{1}{2}}$ and $\bar{q}_{i,j-\frac{1}{2}}$ are defined. By (2.18a) we see that the derivatives of the mapping, at the cell boundaries, are approximated by central differences.

By elementary interpolation theory it can be seen that (2.15) holds (assuming a sufficiently smooth mapping).

We wish to deal with upwind schemes therefore we have to introduce an approximate Riemann-solver or equivalently a numerical flux function. This can be easily done by using the property of rotational invariance of the Euler equations i.e.

$$\cos\phi f(q) + \sin\phi g(q) = T(\phi)^{-1} f(T(\phi)q), \quad (2.19)$$

with

$$T(\phi) = \begin{pmatrix} 1 & 0 & 0 & 0 \\ 0 & \cos\phi & \sin\phi & 0 \\ 0 & -\sin\phi & \cos\phi & 0 \\ 0 & 0 & 0 & 1 \end{pmatrix}, \quad (2.20)$$

and q , $f(q)$ and $g(q)$ as in (2.2), $\phi \in \mathbb{R}$.

Define $l_{i+\frac{1}{2},j}$, $l_{i,j+\frac{1}{2}}$ by

$$l_{i+\frac{1}{2},j} = (y_{\eta_{j+n}}^2 + x_{\eta_{j+n}}^2)^{\frac{1}{2}}, \quad l_{i,j+\frac{1}{2}} = (x_{\xi_{j+n}}^2 + y_{\xi_{j+n}}^2)^{\frac{1}{2}}, \quad (2.21a)$$

and $\phi_{i+\frac{1}{2},j}$, $\phi_{i,j+\frac{1}{2}}$ by

$$\begin{aligned} l_{i+\frac{1}{2},j} \cos\phi_{i+\frac{1}{2},j} &= y_{\eta_{j+n}}, & l_{i+\frac{1}{2},j} \sin\phi_{i+\frac{1}{2},j} &= -x_{\eta_{j+n}}, \\ l_{i,j+\frac{1}{2}} \cos\phi_{i,j+\frac{1}{2}} &= -y_{\xi_{j+n}}, & l_{i,j+\frac{1}{2}} \sin\phi_{i,j+\frac{1}{2}} &= x_{\xi_{j+n}}, \end{aligned} \quad (2.21b)$$

then using (2.19)-(2.21), (2.18) yields

$$\begin{aligned} (\tilde{N}_h q)_{i,j} &= \frac{1}{h} \{ l_{i+\frac{1}{2},j} T_{i+\frac{1}{2},j}^{-1} f(T_{i+\frac{1}{2},j} \bar{q}_{i+\frac{1}{2},j}) - l_{i-\frac{1}{2},j} T_{i-\frac{1}{2},j}^{-1} f(T_{i-\frac{1}{2},j} \bar{q}_{i-\frac{1}{2},j}) \\ &\quad + l_{i,j+\frac{1}{2}} T_{i,j+\frac{1}{2}}^{-1} f(T_{i,j+\frac{1}{2}} \bar{q}_{i,j+\frac{1}{2}}) - l_{i,j-\frac{1}{2}} T_{i,j-\frac{1}{2}}^{-1} f(T_{i,j-\frac{1}{2}} \bar{q}_{i,j-\frac{1}{2}}) \}, \end{aligned} \quad (2.22)$$

where $T_{i+\frac{1}{2},j} = T(\phi_{i+\frac{1}{2},j})$ etc. This formula strongly suggest how to define the first and second order upwind schemes $N_h^p : X_h \rightarrow Y_h$, $p = 1, 2$ namely

$$\begin{aligned} (N_h^p q)_{i,j} &= \frac{1}{h} \{ l_{i+\frac{1}{2},j} T_{i+\frac{1}{2},j}^{-1} f(T_{i+\frac{1}{2},j} q_{i+\frac{1}{2},j}^-, T_{i+\frac{1}{2},j} q_{i+\frac{1}{2},j}^+) - \\ &\quad l_{i-\frac{1}{2},j} T_{i-\frac{1}{2},j}^{-1} f(T_{i-\frac{1}{2},j} q_{i-\frac{1}{2},j}^-, T_{i-\frac{1}{2},j} q_{i-\frac{1}{2},j}^+) + l_{i,j+\frac{1}{2}} T_{i,j+\frac{1}{2}}^{-1} f(T_{i,j+\frac{1}{2}} q_{i,j+\frac{1}{2}}^-, T_{i,j+\frac{1}{2}} q_{i,j+\frac{1}{2}}^+) - \\ &\quad l_{i,j-\frac{1}{2}} T_{i,j-\frac{1}{2}}^{-1} f(T_{i,j-\frac{1}{2}} q_{i,j-\frac{1}{2}}^-, T_{i,j-\frac{1}{2}} q_{i,j-\frac{1}{2}}^+) \}, \end{aligned} \quad (2.23)$$

where

$$\begin{aligned} q_{i+\frac{1}{2},j}^- &= q_{i,j}, \quad q_{i+\frac{1}{2},j}^+ = q_{i+1,j}, \\ q_{i,j}^- &= q_{i,j}, \quad q_{i,j}^+ = q_{i,j+1}, \end{aligned} \quad (2.23a)$$

for the first order approximation ($p=1$) or

$$\begin{aligned} q_{i+\frac{1}{2},j}^- &= q_{i,j} + \frac{1}{2}(q_{i,j} - q_{i-1,j}), \quad q_{i+\frac{1}{2},j}^+ = q_{i+1,j} + \frac{1}{2}(q_{i+1,j} - q_{i+2,j}), \\ q_{i,j}^- &= q_{i,j} + \frac{1}{2}(q_{i,j} - q_{i,j-1}), \quad q_{i,j}^+ = q_{i,j+1} + \frac{1}{2}(q_{i,j+1} - q_{i,j+2}), \end{aligned} \quad (2.23b)$$

for the second order approximation ($p=2$) and $q \in X_h$. Furthermore $f(\cdot, \cdot) : \mathbb{R}^4 \times \mathbb{R}^4 \rightarrow \mathbb{R}^4$ is one of the numerical flux functions found in the literature [5],[11],[12],[13],[15]. For consistency we only need that the numerical flux $f(\cdot, \cdot)$ is consistent with the physical flux i.e.

$$f(q, q) = f(q) \quad (2.24)$$

To proof that $(N_h^p R_h q)_{i,j} - (\bar{N}_h q)_{i,j} = O(h^p)$, $p=1,2$ it is easily seen that we only need to show that for all sufficiently smooth $q \in X$

$$\begin{aligned} \frac{1}{h} \cdot [l_{i+\frac{1}{2},j} T_{i+\frac{1}{2},j}^{-1} \{f(T_{i+\frac{1}{2},j} q_{i+\frac{1}{2},j}^-, T_{i+\frac{1}{2},j} q_{i+\frac{1}{2},j}^+) - f(T_{i+\frac{1}{2},j} \bar{q}_{i+\frac{1}{2},j})\} - \\ l_{i-\frac{1}{2},j} T_{i-\frac{1}{2},j}^{-1} \{f(T_{i-\frac{1}{2},j} q_{i-\frac{1}{2},j}^-, T_{i-\frac{1}{2},j} q_{i-\frac{1}{2},j}^+) - f(T_{i-\frac{1}{2},j} \bar{q}_{i-\frac{1}{2},j})\}] = O(h^p), \end{aligned} \quad (2.25)$$

with the same conventions as in (2.18b) and (2.23); thus $q_{i,j} = (R_h q)_{i,j}$ in (2.23a,b). In order to prove (2.25) first define

$$\bar{q}(\xi, \eta) = \frac{1}{h^2} \int_{\xi - \frac{h}{2}}^{\xi + \frac{h}{2}} \int_{\eta - \frac{h}{2}}^{\eta + \frac{h}{2}} q(\alpha, \beta) d\alpha d\beta, \quad (2.26)$$

then

$$\bar{q}(ih, jh) = \frac{1}{h^2} \int_{\Omega_{i,j}} q(\alpha, \beta) d\alpha d\beta = (R_h q)_{i,j}, \quad (2.27)$$

and

$$\frac{\partial}{\partial \xi} \bar{q}(\xi, \eta) |_{(ih, jh)} = \frac{1}{h} (\bar{q}_{i+\frac{1}{2},j} - \bar{q}_{i-\frac{1}{2},j}). \quad (2.28)$$

From (2.27) and (2.23a,b) we see that

$$\frac{1}{h} (q_{i+\frac{1}{2},j}^\pm - q_{i-\frac{1}{2},j}^\pm) = \frac{\partial}{\partial \xi} \bar{q}(\xi, \eta) |_{(ih, jh)} + O(h^p). \quad (2.29)$$

Thus, using (2.28), (2.29) yields

$$q_{i+\frac{1}{2},j}^\pm - \bar{q}_{i+\frac{1}{2},j} = q_{i-\frac{1}{2},j}^\pm - \bar{q}_{i-\frac{1}{2},j} + O(h^{p+1}). \quad (2.30)$$

Furthermore it is clear that

$$q_{i+\frac{1}{2},j}^\pm - \bar{q}_{i+\frac{1}{2},j} = O(h^p). \quad (2.31)$$

Assuming that the numerical flux function is sufficiently smooth, it follows by a Taylor expansion that

$$\begin{aligned} f(q_{i+\frac{1}{2},j}^-, q_{i+\frac{1}{2},j}^+) &= f(\bar{q}_{i+\frac{1}{2},j}^-, \bar{q}_{i+\frac{1}{2},j}^+) + f'_1(\bar{q}_{i+\frac{1}{2},j}^-, \bar{q}_{i+\frac{1}{2},j}^+) (q_{i+\frac{1}{2},j}^- - \bar{q}_{i+\frac{1}{2},j}^-) + \\ &f'_2(\bar{q}_{i+\frac{1}{2},j}^-, \bar{q}_{i+\frac{1}{2},j}^+) (q_{i+\frac{1}{2},j}^+ - \bar{q}_{i+\frac{1}{2},j}^+) + O(|q_{i+\frac{1}{2},j}^- - \bar{q}_{i+\frac{1}{2},j}^-|^2, |q_{i+\frac{1}{2},j}^+ - \bar{q}_{i+\frac{1}{2},j}^+|^2). \end{aligned} \quad (2.32)$$

Due to the consistency of the numerical flux function and using (2.31), (2.32) yields

$$f(T_{i+\frac{1}{2},j} q_{i+\frac{1}{2},j}^-, T_{i+\frac{1}{2},j} q_{i+\frac{1}{2},j}^+) - f(T_{i+\frac{1}{2},j} \bar{q}_{i+\frac{1}{2},j}) =$$

$$\begin{aligned}
 & f_1 (T_{i+\frac{1}{2},j} \bar{q}_{i+\frac{1}{2},j} , T_{i+\frac{1}{2},j} \bar{q}_{i+\frac{1}{2},j}) \cdot T_{i+\frac{1}{2},j} (q_{i+\frac{1}{2},j}^- - \bar{q}_{i+\frac{1}{2},j}) + \\
 & f_2 (T_{i+\frac{1}{2},j} \bar{q}_{i+\frac{1}{2},j} , T_{i+\frac{1}{2},j} \bar{q}_{i+\frac{1}{2},j}) \cdot T_{i+\frac{1}{2},j} (q_{i+\frac{1}{2},j}^+ - \bar{q}_{i+\frac{1}{2},j}) + O(h^{2p}). \tag{2.33}
 \end{aligned}$$

If the mapping is sufficiently smooth then

$$l_{i+\frac{1}{2},j} - l_{i-\frac{1}{2},j} = O(h) , T_{i+\frac{1}{2},j} - T_{i-\frac{1}{2},j} = O(h) , T_{i+\frac{1}{2},j}^{-1} - T_{i-\frac{1}{2},j}^{-1} = O(h). \tag{2.34}$$

From (2.33),(2.30),(2.31) and (2.34) it is easily derived that (2.25) holds. Hence, N_h^p , $p=1,2$ are p -order accurate approximations of N .

Remarks

-The smoothness of the coordinate transformation (2.5) is necessary to obtain first and second order accurate space discretizations.

-The equation $(N_h^p q)_{i,j} = 0$ is equivalent with $(h^2 N_h^p q)_{i,j} = 0$. After multiplication of (2.23) by h^2 it is clear that $(h^2 N_h^p q)_{i,j}$ is determined completely by the coordinates $\{ (x_{i+\frac{1}{2},j+\frac{1}{2}} , y_{i+\frac{1}{2},j+\frac{1}{2}}) \}$ of the vertices of the mesh in the physical space (and, of course, by the numerical flux function $f(,)$). This means that in the physical space on an irregular mesh, a first and second order finite volume scheme can be constructed without the actual need of a coordinate transformation. The finite volume space discretization on an irregular mesh behaves in a first or second order manner only if the irregular mesh is chosen in accordance with a smooth transformation.

-Consider the steady Euler equations in the computational space $N(q) = 0$ and their discretization $(N_h^p q)_{i,j} = 0$, $p = 1, 2$ (see respectively (2.9),(2.23)). Let $q^p \in X_h$, $p = 1, 2$ denote the solutions of the discrete equations and $q = \tilde{q}(\xi, \eta) \in X$ be the solution of the continuous equation. If the operators N_h^p , $p = 1, 2$ are stable then

$$q_{i,j}^p = \bar{q}_{i,j} + O(h^p) , \tag{2.35}$$

where $\bar{q}_{i,j} = (R_h \tilde{q})_{i,j} = \frac{1}{h^2} \cdot \int \int_{\Omega_{i,j}} \tilde{q}(\xi, \eta) d\xi d\eta$. Define

$$\bar{Q}_{i,j} = \frac{1}{V_{i,j}} \cdot \int \int_{\Omega_{i,j}} \tilde{q}(\xi, \eta) \cdot J(\xi, \eta) d\xi d\eta ,$$

with

$$V_{i,j} = \int \int_{\Omega_{i,j}} J(\xi, \eta) d\xi d\eta .$$

Then $V_{i,j}$ is the area of $\Omega_{i,j}^*$ in the physical space and $\bar{Q}_{i,j}$ is the mean value of $\tilde{q}(x,y)$ in $\Omega_{i,j}^*$. Assuming sufficient smoothness of the Jacobian $J(\xi, \eta)$ it is easily seen that

$$\frac{1}{h^2} \cdot \int \int_{\Omega_{i,j}} J(\xi, \eta) \tilde{q}(\xi, \eta) d\xi d\eta = \frac{1}{h^2} \cdot \int \int_{\Omega_{i,j}} J(\xi, \eta) d\xi d\eta \cdot \frac{1}{h^2} \cdot \int \int_{\Omega_{i,j}} \tilde{q}(\xi, \eta) d\xi d\eta + O(h^2).$$

So, $\bar{Q}_{i,j} = \bar{q}_{i,j} + O(h^2)$ and (2.35) yields $q_{i,j}^p = \bar{Q}_{i,j} + O(h^p)$, $p = 1, 2$. Therefore, $q_{i,j}^p$ may be considered as a p -order accurate approximation of $\bar{q}_{i,j}$ as well as $\bar{Q}_{i,j}$.

-In the literature [16],[4],[1] one encounters generalizations of (2.23b) namely

$$\begin{aligned}
 q_{i+\frac{1}{2},j}^- &= q_{i,j} + \frac{1+\kappa}{4} \cdot (q_{i+1,j} - q_{i,j}) + \frac{1-\kappa}{4} \cdot (q_{i,j} - q_{i-1,j}) , \\
 q_{i+\frac{1}{2},j}^+ &= q_{i+1,j} + \frac{1+\kappa}{4} \cdot (q_{i,j} - q_{i+1,j}) + \frac{1-\kappa}{4} \cdot (q_{i+1,j} - q_{i+2,j}) . \tag{2.36}
 \end{aligned}$$

and similar $q_{i,j+\frac{1}{2}}^\pm$, $\kappa \in [-1, 1]$.

It can be easily seen that (2.29) and (2.31) hold for each κ . Therefore (2.36) results in a second

order accurate space discretization as well as (2.23b).

-Even when $x(\xi, \eta) = \xi$, $y(\xi, \eta) = \eta$ it can be seen that for all smooth $q \in X$

$$(\tilde{N}_h q)_{i,j} - (R_h N q)_{i,j} = O(h^2).$$

So it is plausible that $R_h N$ cannot be approximated more accurately than second order if the flux computation is based on the calculation of constant states at the cell boundaries. This is due to the fact that at a cell boundary the mean flux differs from the flux calculated in the mean state. So this result is typical for 2 and 3 dimensional problems. A formal proof of this result can be given.

3. THE DEFECT CORRECTION METHOD

In section 2 the description of first and second order upwind space discretizations of the 2D steady Euler equations has been given.

In this section the steady Euler equations and their first and second order space discretizations are denoted by

$$N q = r ; N_h^1 q_h = r_h ; N_h^2 q_h = r_h , \quad (3.1)$$

with h the meshsize of the (finest) grid.

Let q_h^{1*} and q_h^{2*} be the solutions of respectively $N_h^1 q_h = r_h$ and $N_h^2 q_h = r_h$. Then q_h^{1*} can be calculated efficiently by the multigrid method. We wish to use the defect correction method and the second order space discretization operator N_h^2 to improve q_h^{1*} .

In a first glance the iterative defect correction (DeC) method seems applicable:

$$\begin{cases} q_h^1 := q_h^{1*} , \\ N_h^1 q_h^{n+1} = N_h^1 q_h^n + (r_h - N_h^2 q_h^n) \quad n = 1, 2, \dots \end{cases} \quad (3.2)$$

Unfortunately, dealing with the steady Euler equations, this iteration process is impractical because of the following reasons:

- Suppose, for the moment, that N , N_h^1 and N_h^2 are linear scalar operators with N_h^1 and N_h^2 first and second order discretizations of N . Then the symbols $N(\omega)$, $N_h^1(\omega)$ and $N_h^2(\omega)$ of respectively N , N_h^1 and N_h^2 are defined by

$$N(e^{i\omega x}) = N(\omega) \cdot e^{i\omega x} ; N_h^{1,2}(e^{i\omega x}) = N_h^{1,2}(\omega) \cdot e^{i\omega x} ,$$

and the accuracy of N_h^1 and N_h^2 can be expressed by

$$N(\omega) - N_h^1(\omega) = O(h^{p_1}) ; N(\omega) - N_h^2(\omega) = O(h^{p_2})$$

(ω fixed).

If we define the error $v_h^n = q_h^{1*} - q_h^n$ then

$$N_h^1 v_h^{n+1} = (N_h^1 - N_h^2) v_h^n .$$

Taking $v_h^n = e^{i\omega x}$ then

$$v_h^{n+1} = \left\{ 1 - \frac{N_h^2(\omega)}{N_h^1(\omega)} \right\} v_h^n .$$

On a fixed grid with $\omega \rightarrow 0$, we see that the amplification factor goes to zero (due to the consistency of N_h^1 and N_h^2). This means that low frequency error components are damped effectively by the iterative DeC method. But for high frequency error components ($\frac{\pi}{2h} \leq \omega \leq \frac{\pi}{h}$) the difference

between $N_h^1(\omega)$ and $N_h^2(\omega)$ can be quite large, causing slow or no convergence of the iteration process. Indeed, dealing with the Euler equations it is a practical experience that (3.2) converges very slowly or even not at all. Thus we may not expect to reach the fixed point q_h^{2*} of (3.2). Therefore it makes no sense to make N_h^2 TVD (by a fluxlimiter) because the TVD property only ensures that q_h^{2*} is wiggle free.

On the other hand, after one defect correction iteration q_h^2 obeys

$$N_h^{dc} q_h^2 := N_h^1 (2N_h^1 - N_h^2)^{-1} N_h^1 q_h^2 = r_h.$$

Let $N_h^{dc}(\omega)$ denote the symbol of N_h^{dc} . Then

$$N_h^{dc}(\omega) = \frac{\{N_h^1(\omega)\}^2}{2N_h^1(\omega) - N_h^2(\omega)},$$

and it is easily seen that

$$\begin{aligned} N(\omega) - N_h^{dc}(\omega) &= \frac{N(\omega) \cdot \{N(\omega) - N_h^2(\omega)\} - \{N(\omega) - N_h^1(\omega)\}^2}{N(\omega) - 2 \cdot \{N(\omega) - N_h^1(\omega)\} + \{N(\omega) - N_h^2(\omega)\}} \\ &= O(h^{\min(2p_1, p_2)}) \end{aligned}$$

Because $p_1 = 1$ and $p_2 = 2$, this implies that N_h^{dc} is a second order space discretization of N . So q_h^2 is a second order accurate approximation. In the same way it can be seen that all q_h^n , $n \geq 2$ are second order accurate approximations. Therefore, one or more DeC iteration steps are sufficient to improve the order of accuracy. This is a well known result which also holds for nonlinear problems [2].

From these arguments it is clear that we will apply the DeC method just a few times (at most four iteration steps). Then we will obtain a second order accurate approximation which suffers from wiggles in the neighbourhood of discontinuities. Because (3.2) starts with the solution of a first order scheme, which is a monotone scheme, we can prevent these wiggles by looking more closely to the correction $\delta q_h^n = q_h^n - q_h^{1*}$. After each iteration in (3.2) we will change δq_h^n , as less as possible, but such that adding the changed correction to q_h^{1*} no new local extrema are created. In this way no wiggles can be introduced. This changing of δq_h^n is in fact a limiting process, therefore we may speak of a limited defect correction process. A simple limited defect correction process is:

step1: $\tilde{q}_h := q_h^{1*}$.

step2:

– Calculate q_h from

$$N_h^1 q_h = N_h^1 \tilde{q}_h + (r_h - N_h^2 \tilde{q}_h). \quad (3.3)$$

– Calculate the correction

$$\delta q_h := q_h - q_h^{1*}, \quad (3.4)$$

and set

$$q_h := q_h^{1*}.$$

Then $q_h + \delta q_h$ is the solution of (3.3). Now change q_h and δq_h by scanning the grid in several directions (for instance from north-east to south-west and vice versa and from north-west to south-east and vice versa) and change the states $q_{h_{i,j}}$ and $\delta q_{h_{i,j}}$ in the visiting control volume $\Omega_{i,j}$ by the following algorithm:

$$q_{h_{i,j}} := q_{h_{i,j}} + \delta q_{h_{i,j}}^{new},$$

$$\delta q_{h_{i,j}} := \delta q_{h_{i,j}} - \delta q_h^{new}{}_{i,j}, \quad (3.5)$$

where

$$\begin{aligned} \delta q_h^{new}{}_{i,j} = & H(\delta q_{h_{i,j}}) \cdot \min(\delta q_{h_{i,j}}, |\delta q_h^+{}_{i,j}|) + \\ & + \{1 - H(\delta q_{h_{i,j}})\} \cdot \max(\delta q_{h_{i,j}}, -|\delta q_h^-{}_{i,j}|), \end{aligned} \quad (3.6)$$

and

$$\begin{aligned} \delta q_h^+{}_{i,j} &:= \max(q_{h_{i-1,j}}, q_{h_{i+1,j}}, q_{h_{i,j-1}}, q_{h_{i,j+1}}) - q_{h_{i,j}}, \\ \delta q_h^-{}_{i,j} &:= \min(q_{h_{i-1,j}}, q_{h_{i+1,j}}, q_{h_{i,j-1}}, q_{h_{i,j+1}}) - q_{h_{i,j}}, \end{aligned} \quad (3.7)$$

and $H : \mathbb{R} \rightarrow \mathbb{R}$ denotes the Heaviside function

$$H(x) = \begin{cases} 1 & \text{if } x > 0 \\ 0 & \text{if } x < 0 \end{cases}.$$

– Finally set $\tilde{q}_h := q_h$.

Formula (3.5)-(3.7) must be applied to each component of $q_{h_{i,j}}$ and $\delta q_{h_{i,j}}$ separately.

It can be easily seen that $\delta q_h^{new}{}_{i,j}$ is a smooth function of $\delta q_{h_{i,j}}$ and $q_{h_{i,j}}$.

Furthermore it is clear that in this way no new local extrema will be introduced in a visiting control volume. Although it is possible that after changing the state in the visiting control volume $\Omega_{i,j}$, a local extrema is created in one of the four neighbouring cells $\Omega_{i\pm 1,j}$, $\Omega_{i,j\pm 1}$. This limiter neglects this possibility, which is expected to occur rarely.

Step2 may be repeated a few times to steepen discontinuities effectively. In general, the limiter will not work in the smooth parts of the flow field, so in those parts the correction δq_h will be added to q_h completely. Only in the neighbourhood of discontinuities this limiter will do its job; preventing oscillations. Therefore this limiter also provides a way to detect discontinuities in the flow field.

4. NUMERICAL RESULTS

The numerical flux function used in these experiments is constructed with Osher's approximate Riemann-solver. Hence, both the first and second order upwind scheme are able to capture shocks and contact discontinuities. To see the improvement of the capturing property after a few DeC iteration steps, two model problems are considered. Problem 1 concerns an oblique shock reflected from a flat plate and problem 2 concerns an oblique contact discontinuity generated by the boundary conditions. The precise description of these two problems is:

Problem1: The oblique shock.

The domain Ω^* is $(0,4) \times (0,1)$. The exact solution has 3 subregions with uniform states as given in figure 4.1.

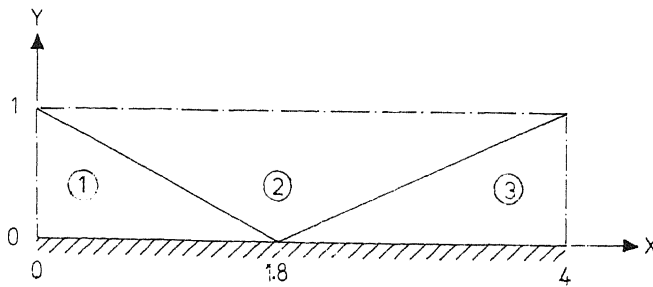


Figure 4.1.

The states are respectively:

state 1: $u = 2.9, v = 0.0, c = 1.0, p = 1.0$,

state 2: $u = 2.6, v = -0.5, c = 1.1, p = 2.1$,

state 3: $u = 2.4, v = 0.0, c = 1.2, p = 4.0$.

Problem2: The contact discontinuity.

Here $\Omega^* = (0,2) \times (0,2)$. The exact solution of the problem has a discontinuity at $x + y = 2$. In both parts of the domain the solution has a uniform state:

for $x + y < 2$ we take $p = 1.0, u = 0.3, v = -0.3, c = 0.6$,

for $x + y > 2$ we take $p = 1.0, u = 0.6, v = -0.6, c = 1.0$.

For the treatment of the boundary conditions see [7].

The figures 1,2,3 and 4 concern the resolution of the oblique shock and the figures 5 and 6 of the contact discontinuity.

Figure 1a,1b and 1c show the pressure contours on a 8×24 mesh, respectively obtained by the first order Osher scheme and after 1 and 4 DeC iteration steps. Figure 2a,2b and 2c show the same results but on a 16×48 mesh. In all cases the limiter, described in section 3, has been used. In figure 3a and 3b pressure distributions along the flat plate are shown (using the 16×48 mesh). In these figures results are shown, again obtained by the first order scheme and after 1 and 4 DeC iterations. Figure 3a has been obtained with, figure 3b without the limiter. Figure 4a and 4b show similar results at $y = 0.5$. After 4 DeC iteration steps the quality of the shock capturing seems comparable with the results obtained by a second order TVD scheme [3].

Figure 5a,5b,5c and 6a,6b,6c show density contours on respectively a 16×16 and a 32×32 mesh. Again results of the first order scheme and after 1 and 4 DeC iteration steps are shown. For comparison see [7].

For both problems, it is clear that after a few DeC iteration steps the capturing of the discontinuities has been improved considerably.

5. CONCLUSION

This paper is concerned with the discretization of the steady Euler equations by the finite volume technique. On an irregular mesh it is shown in detail how to apply Van Leer's projection-evolution stages in the discretization. Herein, the rotational invariance of the Euler equations is effectively used. For a general numerical flux function, consistent with the physical flux, a proof is given of the order of accuracy for a first and second order upwind scheme. Hence, the results hold for all well known approximate Riemann-solvers.

Second order accurate approximations are obtained by a defect correction (DeC) method. A limiter, used in the DeC method, is constructed to maintain monotone solutions. For two typical model problems (an oblique shock and a contact discontinuity), only a few (3 or 4) DeC iteration steps are

sufficient to steepen discontinuities effectively. This makes the method cheap to apply. Furthermore, the quality of the results seems comparable with results obtained by TVD schemes.

Acknowledgement. The author would like to thank P.W.Hemker, B.Koren and P.M.de Zeeuw for their cooperation and valuable suggestions.

REFERENCES

- [1] Anderson, W.T., Thomas, J.L., and Van Leer, B., "A comparison of finite volume flux vector splittings for the Euler equations" AIAA Paper No. 850122.
- [2] Böhmer, K., Hemker, P. & Stetter, H., "The Defect Correction Approach." Computing Suppl. 5 (1984) 1-32.
- [3] Chakravarthy, S.R. and Osher, S., "High resolution applications of the Osher upwind scheme for the Euler equations." AIAA Paper 83-1943, Proc. AIAA Sixth Computational Fluid Dynamics Conf. (Danvers, Mass. July 1983), 1983, pp 363-372.
- [4] Chakravarthy, S.R. and Osher, S., "A new class of high accuracy TVD schemes for hyperbolic conservation laws." AIAA Paper 85-0363, AIAA 23rd Aerospace Science Meeting. (Jan. 14-17, 1985/Reno, Nevada).
- [5] Godunov, S.K., "A finite difference method for the numerical computation of discontinuous solutions of the equations of fluid dynamics." Mat.Sb.(N.S.)47(1959),271-; also Cornell Aeronautical Laboratory transl.
- [6] Harten, A., Lax, P.D. & Van Leer, B., "On upstream differencing and Godunov-type schemes for hyperbolic conservation laws." SIAM Review 25 (1983) 35-61.
- [7] Hemker, P.W., "Defect correction and higher order schemes for the multi grid solution of the steady Euler equations." In this volume.
- [8] Hemker, P.W. & Spekreijse, S.P., "Multigrid solution of the Steady Euler Equations." In: Advances in Multi-Grid Methods (D.Braess, W.Hackbusch and U.Trottenberg eds) Proceedings Oberwolfach Meeting, Dec. 1984, Notes on Numerical Fluid Dynamics, Vol.11, Vieweg, Braunschweig, 1985.
- [9] Hemker, P.W. & Spekreijse, S.P., "Multiple Grid and Osher's Scheme for the Efficient Solution of the Steady Euler Equations." Report NM-8507, CWI, Amsterdam, 1985.
- [10] Mulder, W.A. "Multigrid Relaxation for the Euler equations." To appear in: J. Comp. Phys. 1985.
- [11] Osher, S & Solomon, F., "Upwind difference schemes for hyperbolic systems of conservation laws." Math. Comp. 38 (1982) 339-374.
- [12] Roe, P.L., "Approximate Riemann solvers, parameter vectors and difference schemes." J. Comp. Phys. 43 (1981) 357-372.
- [13] Steger, J.L. & Warming, R.F., "Flux vector splitting of the inviscid gasdynamics equations with applications to finite difference methods." J. Comp. Phys. 40 (1981) 263-293.
- [14] Sweby, P.K. "High resolution schemes using flux limiters for hyperbolic conservation laws", SIAM J.Numer.Anal. 21 (1984) 995-1011.
- [15] Van Leer, B., "Flux-vector splitting for the Euler equations." In: Procs. 8th Intern. Conf. on numerical methods in fluid dynamics, Aachen, June, 1982. Lecture Notes in Physics 170, Springer Verlag.
- [16] Van Leer, B., "Upwind difference methods for aerodynamic problems governed by the Euler equations." Report 84-23, Dept. Math. & Inf., Delft Univ. Techn., 1984.
- [17] Van Leer, B., "Towards the ultimate conservative difference scheme.2. Monotonicity and conservation combined in a second order scheme." J.Comp.Phys.14,361-370(1974).
- [18] Van Leer, B. & Mulder, W.A., "Relaxation methods for hyperbolic equations." Report 84-20, Dept. Math. & Inf., Delft Univ. Techn., 1984.

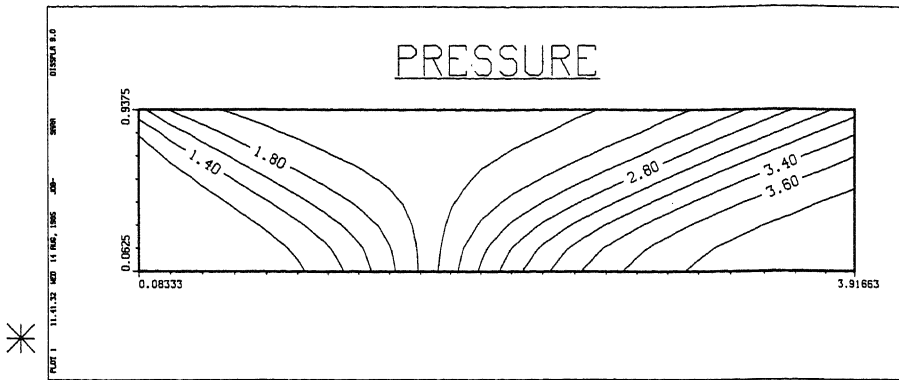


Figure 1a.

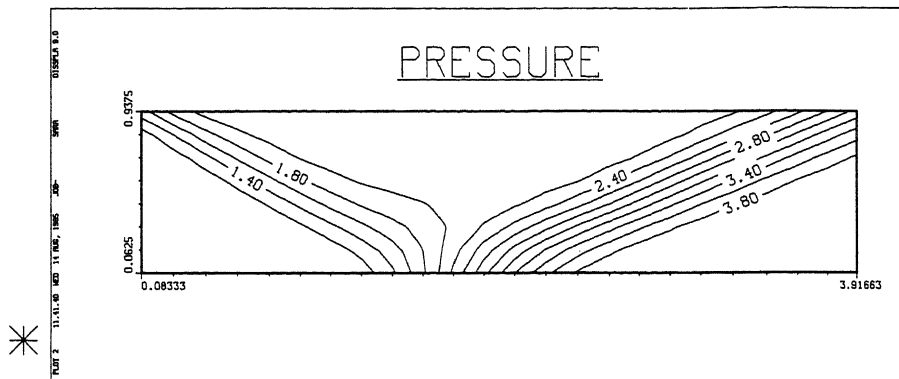


Figure 1b.

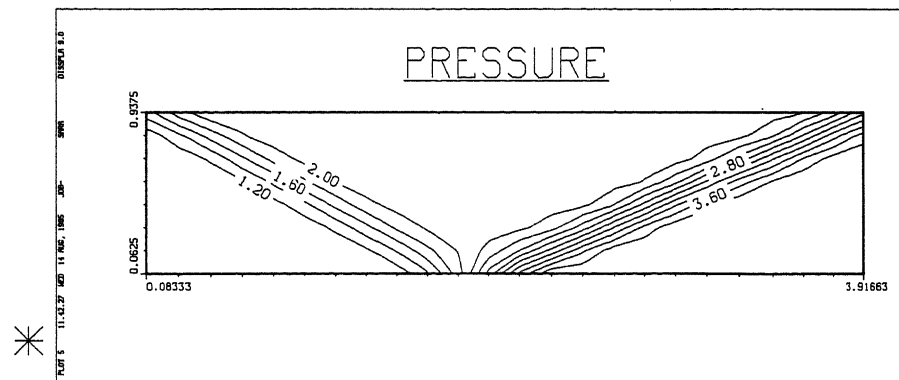


Figure 1c.

Pressure contours of an oblique shock on a 8×24 mesh, obtained by the first order upwind scheme and after 1 and 4 DeC iteration steps.

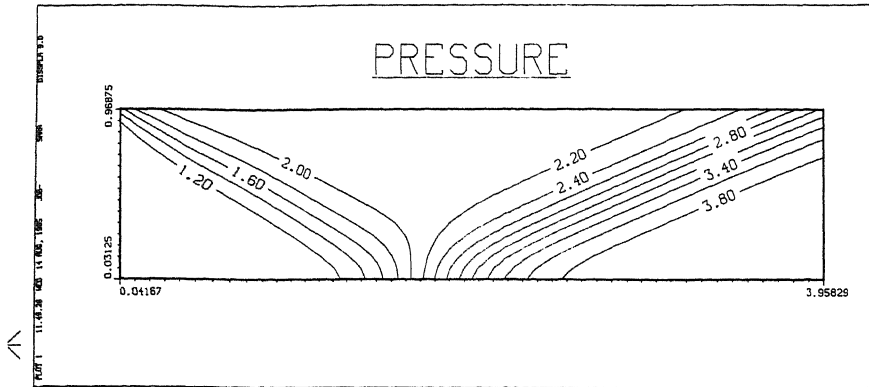


Figure 2a.

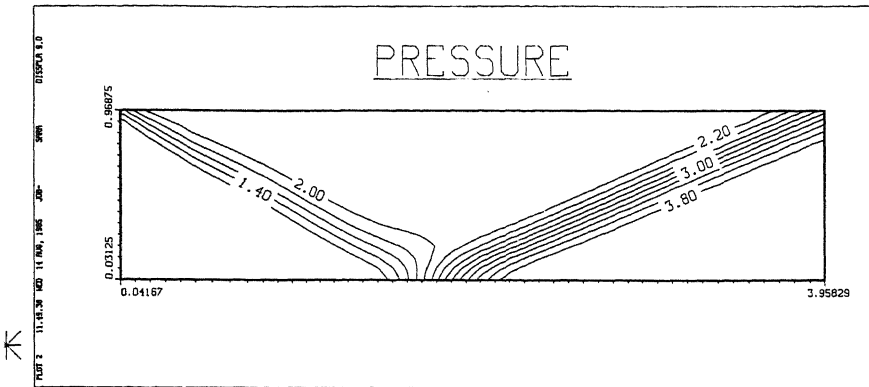


Figure 2b.

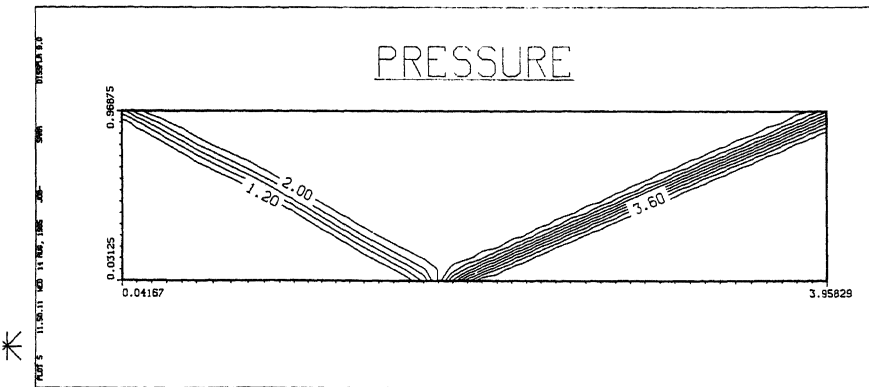


Figure 2c.

Pressure contours on a 16×48 mesh.

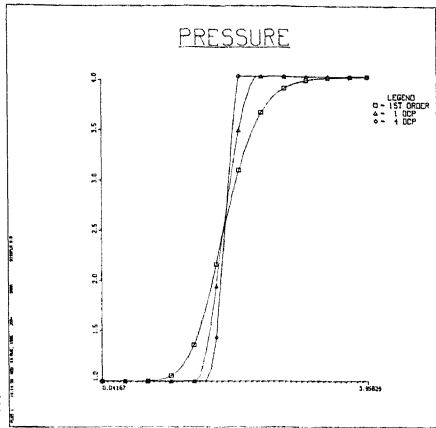


Figure 3a.

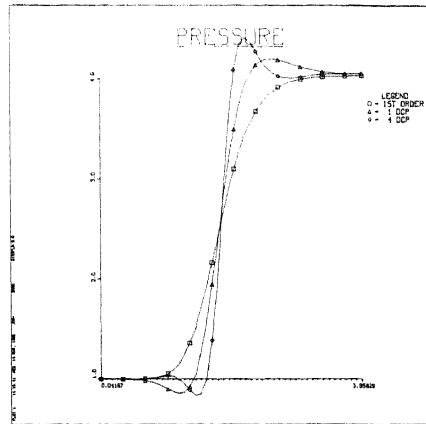


Figure 3b.

Pressure profiles computed at the surface of the flat plate, using the first order scheme and after 1 and 4 DeC iteration steps. Figure 3a has been obtained with a limiter, figure 3b without.

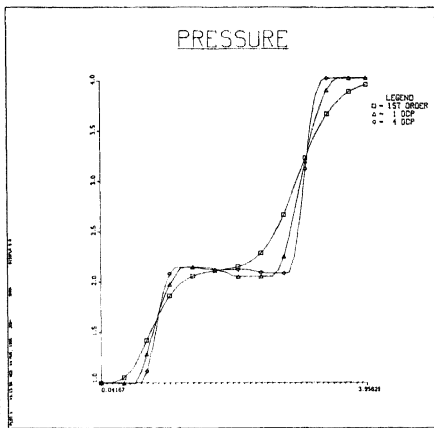


Figure 4a.

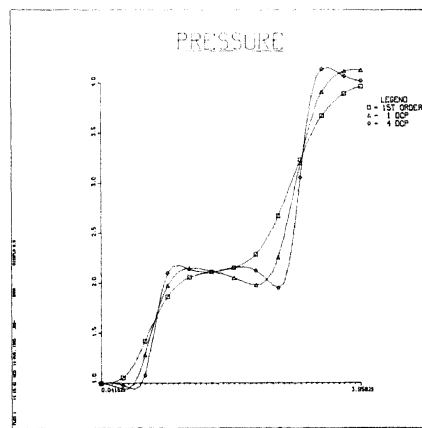


Figure 4b.

Pressure profiles at $y=0.5$.

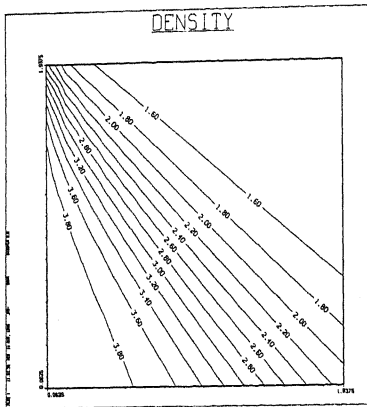


Figure 5a.

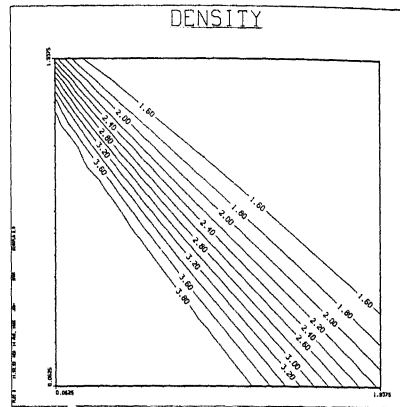


Figure 5b.

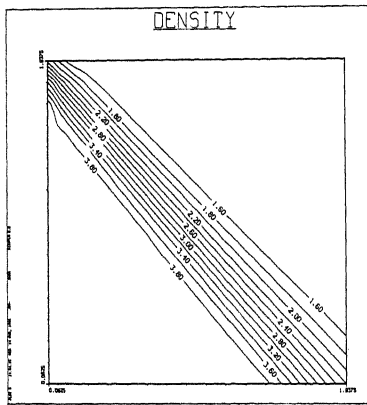


Figure 5c.

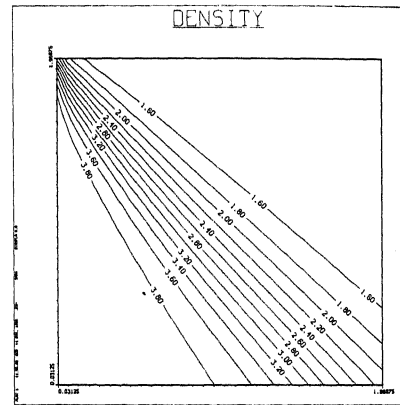


Figure 6a.

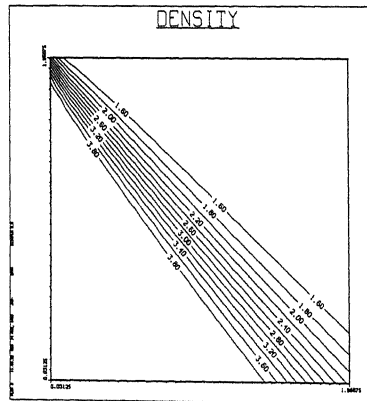


Figure 6b.

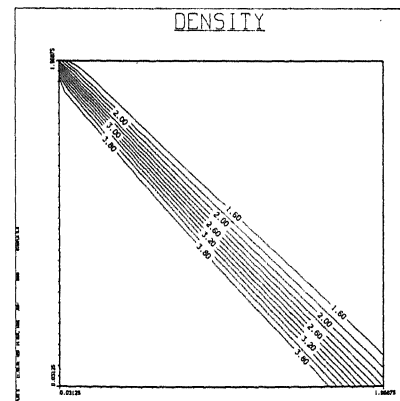


Figure 6c.

Density contours of a contact discontinuity on a 16×16 (figure 5) and a 32×32 (figure 6) mesh, obtained by the first order scheme and after 1 and 4 DeC iteration steps.